# Universal scaling law of electrical turbulence in the mammalian heart

Sami F. Noujaim[†], Omer Berenfeld[†], Jérôme Kalifa[†], Marina Cerrone[†], Kumaraswamy Nanthakumar[‡], Felipe Atienza[§], Javier Moreno[¶], Sergey Mironov[†], and José Jalife[†‖]

[†]Department of Pharmacology and Institute for Cardiovascular Research, SUNY Upstate Medical University, Syracuse, NY 13210; [‡]Division of Cardiology, Toronto General Hospital, Toronto, ON, Canada M5G 2C4; [§]Hospital General Universitario Gregorio Marañon, 28007 Madrid, Spain; and [¶]Cardiovascular Institute, Hospital Clinico San Carlos, 28040 Madrid, Spain

Communicated by Charles S. Peskin, New York University, New York, NY, October 13, 2007 (received for review April 18, 2007)

**Many biological processes, such as metabolic rate and life span, scale with body mass (BM) according to the universal law of allometric scaling: $Y = aBM^b$ ($Y$, biological process; $b$, scaling exponent). We investigated whether the temporal properties of ventricular fibrillation (VF), the major cause of sudden and unexpected cardiac death, scale with BM. By using high-resolution optical mapping, numerical simulations and metaanalysis of VF data in 11 mammalian species, we demonstrate that the interbeat interval of VF scales as $VF_{cycle\ length} = 53 \times BM^{1/4}$, spanning more than four orders of magnitude in BM from mouse to horse.**

allometry | spiral waves | ventricular fibrillation

Ventricular fibrillation (VF) is an extremely abnormal heart rhythm that impedes blood pumping to the brain and vital organs, resulting in sudden death (1). VF has been described as turbulent cardiac electrical activity, and several hypotheses have been put forth to explain the very complex electrical behavior that characterizes it. One school of thought suggests that, during fibrillation, the electrical waves propagate through the ventricles at random, with no underlying deterministic organization (2, 3). Others postulate that, although VF is complex, it is maintained by organized electrical vortices, called "rotors," that spin at exceedingly high frequencies around a central core region (4). Waves shed by the rotors take a spiral shape near the core but may turn into disorganized patterns of propagation known as "fibrillatory conduction" in the rotor's periphery (4). Based on normal electrophysiology and anatomy, it is suggested that all mammalian hearts are built on the same template (5), and fibrillation has been shown to occur in the hearts of all mammalian species studied to date, from the mouse to the horse. The question therefore arises as to whether the spatiotemporal properties of VF scale with body mass (BM). More specifically, are rotors spinning at high frequency the universal mechanism of sudden death due to VF?

Many biological processes such as metabolic rate, life span, and respiratory rate do scale with BM according to the universal law of allometric scaling: $Y = aBM^b$, where $Y$ is the biological process, and $b$ is the scaling exponent, that often is a multiple of 1/4 (6). It has been proposed, using metabolic rate (MR) scaling ($MR \propto BM^{3/4}$), that the underlying mechanism of the 1/4 power law is an evolutionary means to optimize biological systems brought about by the maximization of exchange surface areas and the minimization of transport distances and times (6, 7).

Cardiovascular variables have been predicted and shown to scale with BM as well. For example, in the ECG of the mammalian heart, the time intervals that define the normal interbeat interval (RR), atrioventricular conduction (PR), duration of ventricular activation (QRS), and duration of the excited state (QT) are all proportional to $BM^{1/4}$ (5, 6, 8–10). It was recently proposed that the PR interval is $\propto BM^{1/4}$ because of the delivery of the action potential from the sinoatrial node, to the ventricles, and through a branching self-similar network (the specialized conduction system) (8). Consequently, it is established that the propagation of the electrical impulse from the atria to the ventricles in the mammalian heart depends on body size. Of note is the left ventricular ejection time, which is $\propto BM^{1/4}$ (11), suggesting that, across mammalian species, the normal electrical makeup of the heart is tightly coupled to its pumping function. However, it remains unknown whether the abnormal electrical wave propagation that characterizes VF holds a relation of dependence on BM.

## Results and Discussion

**Electrical Excitation During the Normal Heartbeat.** Each heartbeat is preceded by an electrical excitation wave that propagates through the atrial and ventricular myocardium. The diagram in Fig. 1*A* depicts the normal sequence of endocardial electrical activation of the mammalian heart during sinus rhythm. The cardiac impulse is generated by the natural pacemaker, the sinoatrial node (SN). Under normal conditions, after the atria are activated, the impulse does not propagate directly into the ventricles but must proceed slowly through the atrioventricular node (AVN) and then the His bundle, where it accelerates to move at a high speed through the right and left bundle branches and the Purkinje cell network of the specialized conduction system (shown in red in Fig. 1*A*). The impulse then excites both ventricles, from endocardium to epicardium. As shown in Fig. 1*B*, two quasi-simultaneous wave fronts break through the epicardium on the free walls of the right and left ventricles. These waves subsequently merge to activate the rest of the ventricular myocardium. The patterns of wave spread observed here in representative mouse and pig hearts are nearly identical to that in the human heart (12) and are required to effectively trigger the synchronous contraction of both ventricles for the ejection of blood at a high pressure. Synchronous excitation is thus an essential component of the heart's functioning as a pump.

**Electrical Excitation During Ventricular Fibrillation.** During VF, the ventricular activation sequence is profoundly abnormal; electrical wavefronts no longer follow the usual paths. The heart rate accelerates to the extreme, and the electrical waves assume a complex vortex-like behavior that brings to mind eddy formation and turbulence in water. Such turbulence renders the heart unable to pump blood. Thus, the blood pressure drops, and immediate loss of consciousness follows. Fibrillatory behavior is illustrated by the data in Fig. 2, which was obtained by high-resolution optical mapping of Langendorff-perfused hearts from four different mammals. We used a fluorescent voltage-sensitive dye and a CCD camera that was focused on the anterior ventricular surface. Snapshots taken from phase movies of wave-propagation dynamics during stable VF reveal sustained vortices (rotors) whose rotation

Author contributions: S.F.N. and O.B. contributed equally to this work; S.F.N., O.B., and J.J. designed research; S.F.N., O.B., J.K., M.C., K.N., F.A., and J.M. performed research; S.F.N., O.B., S.M., and J.J. analyzed data; and S.F.N., O.B., and J.J. wrote the paper.

The authors declare no conflict of interest.

‖To whom correspondence should be addressed. E-mail: jalifej@upstate.edu.

This article contains supporting information online at www.pnas.org/cgi/content/full/0709758104/DC1.

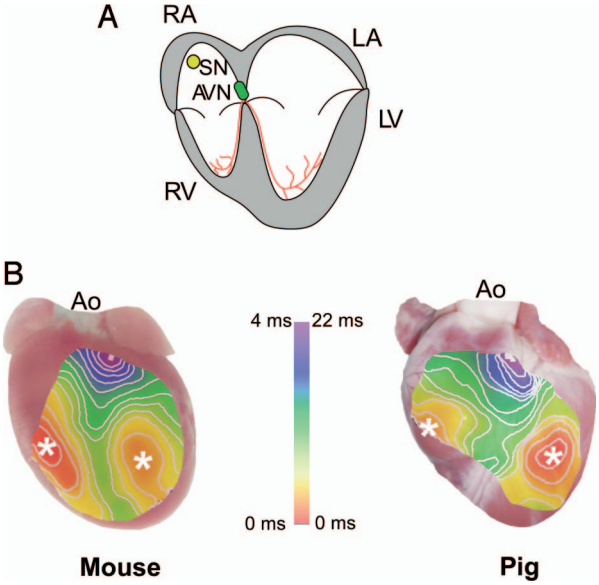


**Fig. 1.** Normal sequence of electrical activation in the mammalian heart. (*A*) Diagram showing endocardial view of the atria and ventricles. Shown in yellow is the sinoatrial node (SN) in the right atrium. The atrioventricular node (AVN) is shown in green. The His–Purkinje system is shown in red, terminating with its branches on the endocardium of the right and left ventricles (RV and LV, respectively). (*B*) Epicardial electrical activation pattern of mouse and pig hearts during normal sinus rhythm. The colored activation maps are superimposed on the digital pictures of the hearts, positioned in the same manner as in *A*. The pattern of ventricular activation is similar in the mouse and pig hearts. Two initial breakthroughs (white asterisks) appear on the LV and RV walls, after which the excitation spreads to the rest of the heart. The white lines are isochrones (0.3 ms for the mouse and 1.5 ms for the pig). The color scale indicates red as the earliest (0 ms) and purple as the latest (4 ms for the mouse and 22 ms for the pig) times of activation. RA, right atrium; Ao, aorta; LA, left atrium.

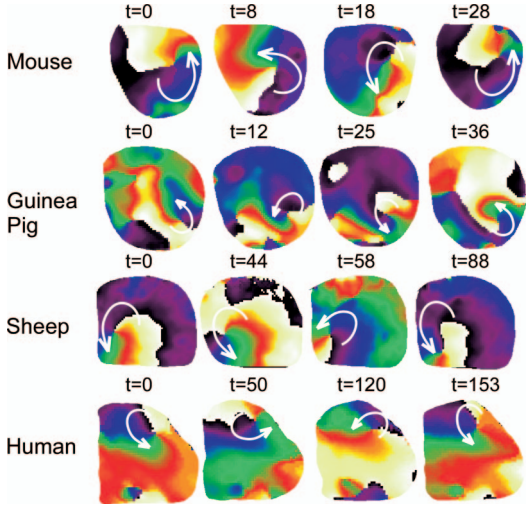


**Fig. 2.** Stable VF in the hearts of four different mammals, from mouse to man. Four action-potential-phase snapshots depict a rotation of spirals in mouse, guinea pig, sheep, and human hearts. Vortex-like reentry is apparent in all hearts. The white circular arrows mark the location of the center and the direction of rotation. Numbers above each map represent time in milliseconds after an arbitrary zero.

frequency depends on the species (mouse, 38 Hz; guinea pig, 26 Hz; sheep, 12 Hz; human, 6.8 Hz).

Fig. 3*A* shows dominant frequency (DF) maps of VF obtained by high resolution fast Fourier transform (FFT) analysis of the optical signals in examples taken from four different species (mouse, guinea pig, rabbit, and human) spanning 3 orders of magnitude in BM. Altogether, these data demonstrate that during VF the ventricles do not activate in synchrony. Some areas excite at higher rates than others and the DFs organize in clearly demarcated domains. As demonstrated in hearts from guinea pigs and mice (4, 13), the frequency of the vortices, or their rotation period (1/frequency), closely matched the frequency of fibrillation or cycle length calculated from the DF maps or the ECG. However, please note that the highest DF domain decreases with increasing body size (mouse, 38 Hz; guinea pig, 26 Hz; rabbit, 15 Hz; human, 6.8 Hz).

**Scaling of Ventricular Fibrillation Frequency.** To establish whether VF frequency actually scales with BM we obtained data from 11 species, ranging from the 30-g mouse to the 400-kg horse in 40 different published studies, as well as in additional studies we performed in mouse, pig, and sheep hearts. When the frequency of fibrillation is plotted against BM on a double logarithmic scale, the best linear fit yields an intercept of $2.95 \pm 0.04$ and a slope of $-0.23 \pm 0.014$ ($R = -0.93$, $P < 0.01$; Fig. 3*B*). It follows that the frequency of VF $\approx 18.9 \cdot \mathrm{BM}^{-1/4}$, and that the interbeat interval of VF $\approx 53 \cdot \mathrm{BM}^{1/4}$.

The plot in Fig. 3 shows that there is variability in the frequency of VF in relation to $\mathrm{BM}^{1/4}$. Because most of these values were collected from the literature, inherent differences in the experimental conditions are likely to be present. Also, fundamental chamber-specific differences in gene expression may contribute to such deviations. For example, in the mouse heart, there are regional differences in the distribution of the Kv1.4 gene responsible for the transient outward potassium current (14), which is known to be more pronounced in mouse than in guinea pig heart (15). However, expression of the inwardly rectifying potassium current is chamber-specific in the guinea pig heart (4). The delayed rectifier potassium current is negligible in the rabbit and rat, but not in the guinea pig and human hearts (15, 16). Such differences in ion channel expression/distribution may significantly affect the frequency and organization of VF. Then again, frequency itself is likely to control VF organization: the higher the frequency, the lower the degree of organization, which helps to explain why VF in human, being slower, seems more organized than in other species (17, 18). Finally, the different organizational pattern of VF in diverse species has been shown to depend on the "effective" size of the heart (19).

The scaling of the interbeat interval of VF with $\mathrm{BM}^{1/4}$ is consistent with the scaling of many physiological time intervals in normal biology, including cardiac cycle, respiratory cycle, life span, total blood circulation time, gestation time, etc., all of which have been shown to be $\propto \mathrm{BM}^{1/4}$ (10). However, here we demonstrate that the interbeat interval of VF, a time scale incompatible with life and a cause of death also follows the same trend, spanning four orders of magnitude in BM.

Although still disputed (20), metabolic rate is widely considered to be $\propto \mathrm{BM}^{3/4}$. The specific metabolic rate ($P^*$) scales $\propto \mathrm{BM}^{-1/4}$, indicating that per unit mass, mouse tissue is energetically more demanding to maintain than human or horse tissue. Indeed, the larger surface-to-volume ratio of smaller mammals enhances heat loss from the body to the environment and suggests the need for an increase in energy utilization to maintain constant biological body temperature (5, 10). Consequently, the density of mitochondria in mouse cells is larger than in cells of bigger mammals and also obeys the same scaling relation with BM as $P^*$ (21). For the cardiovascular system to meet the metabolic demands of the whole organism of a small mammal like the mouse, a higher $P^*$, and consequently higher specific $O_2$ consumption ($\dot{O}_2$), is satisfied by higher heart and breathing rates (*HR* and *BR*, respectively) than in larger animals

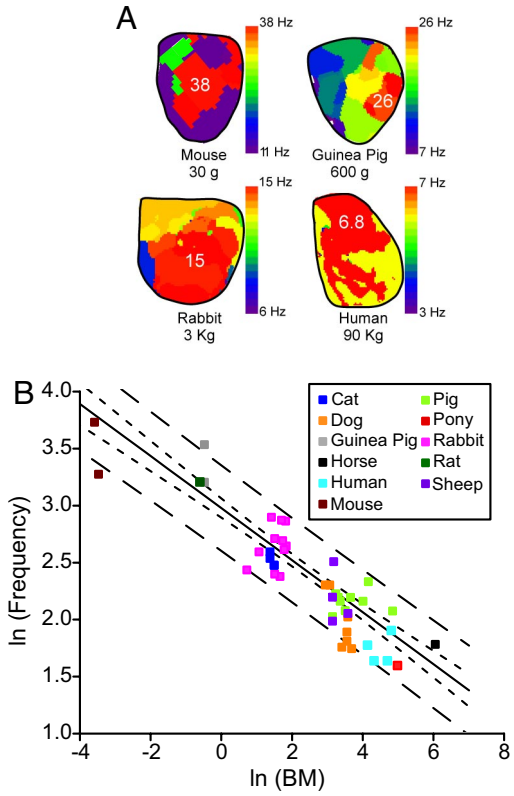


**Fig. 3.** Scaling of VF frequency in mammalian hearts. (*A*) DF maps of epicardial electrical activity of mouse, guinea pig, rabbit, and human hearts during VF. The frequencies of excitation are distributed in clearly demarcated domains. The fastest domain in the mouse heart is 38 Hz, in the guinea pig heart is 26 Hz, in the rabbit heart is15 Hz, and in the human heart is 6.8 Hz. (*B*) Double logarithmic plot of frequency vs. BM covering 11 species, from mouse to horse. Best fit line: $y = 2.94 \pm 0.04 - 0.23x \pm 0.014$; $r = -0.93$; $P < 0.01$. Solid black line indicates best fit, short dashed lines indicate 95% confidence limits, and long dashed lines indicate 95% prediction limits.

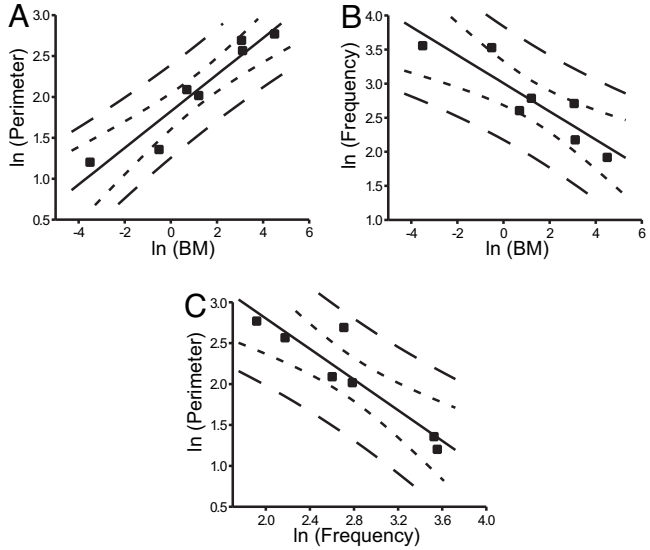


**Fig. 4.** Core perimeter, VF frequency, and BM in mouse, rat, guinea pig, rabbit, sheep, pig, and human hearts. (*A*) ln(core perimeter) vs. ln(BM): $y = 1.82 \pm 0.09 + 0.22x \pm 0.03$; $r = 0.96$; $P < 0.01$. (*B*) ln(frequency) vs. ln(BM): $y = 3 \pm 0.13 - 0.21x \pm 0.05$; $r = -0.9$; $P < 0.01$. (*C*) ln(core perimeter) vs. ln(frequency): $y = 4.67 \pm 0.5 - 0.94x \pm 0.18$; $r = -0.92$; $P < 0.01$. Solid black lines indicates best fit, short dashed lines indicate 95% confidence limits, and long dashed lines indicate 95% prediction limits.

such as the elephant: The *HR* of the mouse is ≈700 beats per minute, and that of the elephant is ≈35 beats per minute. Therefore, it is not surprising that $P^* \propto O_2^{'} \propto BR \propto HR \propto \mathrm{BM}^{-1/4}$ as well.

**Scaling of Rotor Core Size.** Previously, ventricular tachycardia and VF were attributed to rotors spinning with invariant angular velocity around a core of characteristic size (22). Recent data, however, suggest that the core size may be different in different species (13, 23, 24). We therefore investigated the effect of body size on the core perimeter, with the idea of investigating the underlying basis of VF frequency scaling. Under otherwise similar conditions, the core perimeter can be proportional to the product of rotation period ($T$) times conduction velocity, but because conduction velocity is constant across species (25), then the perimeter of the core should scale as $T \propto \mathrm{BM}^{1/4}$. To verify this experimentally, the core perimeters of rotors in fibrillating ventricles of mice, rats, guinea pigs, rabbits, sheep, pigs, and human hearts were assessed. The best linear fit to the logarithmic plot of core perimeter vs. BM was $y = 1.82 \pm 0.09 + 0.22x \pm 0.03$, $r = 0.96$, $P < 0.01$ (Fig. 4*A*). Also, the best-fit line of the logarithmic plot of VF frequency in these experiments vs. BM was $y = 3 \pm 0.13 - 0.21x \pm 0.05$, $r = -0.9$, $P < 0.01$ (Fig. 4*B*). Moreover, when the log of the core perimeter was plotted against the log of VF frequency, the best linear fit had a slope of $-0.94 \pm 0.18$, $r = -0.92$, $P < 0.01$ (Fig. 4*C*).

**Mechanism of Ventricular Fibrillation Scaling.** The question remains as to the mechanism(s) underlying the scaling of core size and VF frequency as $\mathrm{BM}^{1/4}$. Under normal conditions, in order for the mouse heart to beat much faster than the elephant heart, not only its energetic demand must be met but also the entire electrical excitation–recovery cycle; i.e., the action potential duration (APD) must accommodate appropriately to allow fast beating rates (26). If the APD is too long, then when the next impulse arrives, it will find the tissue ahead of it refractory, and thus unexcitable, leading to failure of propagation. If the APD is too short, then the excitation–contraction coupling phenomenon will be compromised, jeopardizing cardiac function. On ECG, the QT interval measures the global electrical activation–recovery cycle of the ventricles. QT scales in proportion to $\mathrm{BM}^{1/4}$ (9). It therefore follows that the APD of the ventricular cells is also $\propto \mathrm{BM}^{1/4}$. It is important to stress that although the above energetic demand argument does not hold for VF, during which ventricular contraction is asynchronous and force generated is negligible after each excitation, it is clear that APD does change with body size and VF frequency.

Given the constant conduction velocity of action potential propagation in mammalian hearts (25) and the scaling of the QT interval during sinus rhythm and VF cycle length to $\mathrm{BM}^{1/4}$, we propose that the rotors that maintain VF from small to large animals spin at periods that are strongly dependent on APD. Our premise here is that as the APD increases, the frequency of VF decreases. To validate such a premise, and to authenticate the postulate that the scaling exponent of VF frequency vs. BM is $-1/4$, we carried out computer simulations of vortex-like reentry in five imaginary species with characteristic heart sizes, $L = 1$, 2, 4, 8, and 16 cm, covering three orders of magnitude in body size (i.e., BM = 0.017–68 kg). We assumed that the density of these hearts is equal to that of water (1g/cm$^3$) and that their total mass represents 0.6% of the BM (5); consequently, $\mathrm{BM} = L^3/0.006$ (27). The cell size was assumed to be invariant across species along with the universal formalism of their simple excitation and recovery, for which we used FitzHugh–Nagumo type membrane kinetics [see supporting information (SI) for details]. The membrane model parameters, however, were adjusted for each species; the time constant and repolarization

PHYSIOLOGY

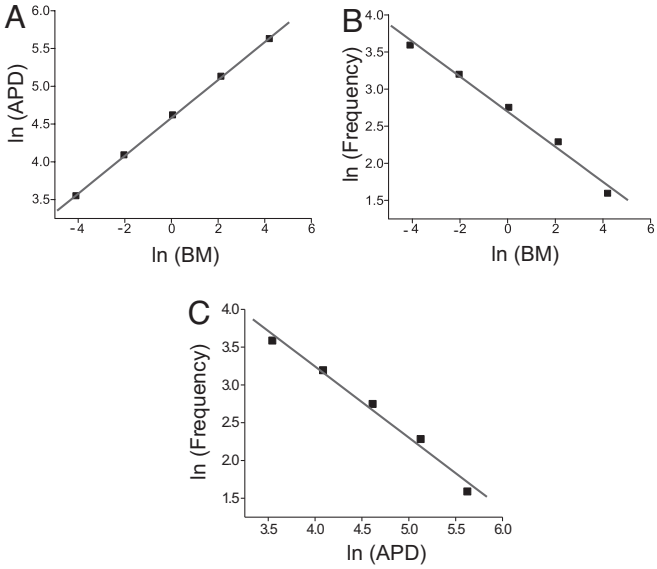


**Fig. 5.** APD and rotor frequency in computer simulations of imaginary species' hearts. (*A*) ln(APD) vs. ln(BM): $y = 4.58 \pm 0.008 + 0.25x \pm 0.003$; $r = 1$; $P < 0.01$. (*B*) ln(frequency) vs. ln(BM): $y = 2.7 \pm 0.05 - 0.24x \pm 0.02$; $r = -0.99$; $P < 0.01$. (*C*) ln(frequency) vs. ln(APD): $y = 7 \pm 0.3 - 0.94x \pm 0.7$; $r = -0.99$; $P < 0.01$. Gray lines indicate best fit.

parameters were scaled such that the APD of each model was close to the realistic values of the species and scale precisely as $BM^{1/4}$ (Fig. 5*A*), while maintaining a fixed plane wave conduction velocity across all species (please see SI). This operation yielded vortices whose frequency of rotation was $\propto BM^{-1/4}$ (Fig. 5*B*) and $\propto APD^{-1}$ (Fig. 5*C*). Although somewhat simplistic, these simulations demonstrate that, in general, one can obtain rotors whose frequencies scale like the VF frequencies with a $-1/4$ exponent by scaling the action potential duration similarly to the QT interval, which in turn is proportional to the BM with a 1/4 exponent (9). The experimentally determined best fit for ln (DF) vs. ln (BM) ($2.94 - 0.23x$) is very close to that determined theoretically from the computer model ($2.7 - 0.24x$).

**What Is the Significance of VF Frequency Scaling?** VF is the leading immediate cause of sudden cardiac death in the industrialized world. It accounts for an estimated 300,000 fatalities annually in the U.S. alone. Yet, despite more than a century of conjecture and experimentation, the mechanisms that initiate and maintain this fatal arrhythmia remain far from being understood. As such, the ability to identify patients at risk as well as preventing VF remains awfully inadequate. The mechanisms of initiation and maintenance of cardiac fibrillation have traditionally been studied using large animal models and numerical simulations. Work from many laboratories has led to the conviction that the onset of fibrillation occurs when an electrical wave first breaks and begins to rotate at an exceedingly high frequency; it escalates into full fibrillation as the wavefronts generated by rotors encounter tissue that is not ready for excitation, and more wave breaks occur, leading to completely irregular excitation. Yet, what are the electrical conditions leading to that wavebreak, and how it can be prevented? We simply do not know. In recent years, transgenic and knockout mouse models have become essential for the elucidation/establishment of general principles underlying cardiac channel diseases and their electrophysiologic and arrhythmogenic consequences. This makes allometric scaling relationships essential when it comes to translating the findings to the clinical setting. Mice and other small mammals are used in research due to their size, short life spans, and affordability, with a supposed correlation between their metabolic and organ function to that of humans. Mouse models have become particularly important as newer inroads into cardiac genomics, proteomics and phenomics hold the promise of defining, at the molecular, cellular and systemic levels, the functional roles of ion channels and their regulation in the mechanisms of VF and sudden cardiac death.

Here we show that, measured in internal clock time, VF is the same in all mammals. The demonstration of such universality in VF dynamics may lead to further studies aimed at achieving a more thoughtful understanding of the fundamental mechanisms of rotor behavior and VF. Thus, important questions pertinent to cardiac function and VF can now be addressed. For example, is there a link between mammalian body size and the assembly of the membrane and intracellular proteins responsible for generating the cardiac electrical waveform? Is there a quantifiable relationship between body size and the expression patterns of genes coding for the cardiac ion channels and signaling molecules involved in cardiac excitation and propagation? Does metabolic rate or environmental factors modulate the molecular organization and electrical properties of the hearts of mammals of different sizes and species? If so, what are the underlying evolutionary factors? Such studies could help pave the way for investigating gene products that may be universally important for initiating/maintaining VF. Should such proteins be identified, they may become the targets for new generations of more effective and safer antiarrhythmic approaches capable of preventing sudden cardiac death (28, 29).

Thus, although the appropriate rendition of the molecular underpinnings of fatal arrhythmias from small mammals to humans is still incomplete, our demonstration that the interbeat interval of VF scales as $BM^{1/4}$ suggests that there might be a strong similarity in the underlying mechanisms of VF in most, if not all, mammalian species, which may be of considerable fundamental and practical significance.

## Materials and Methods

BM, dominant frequency (DF) of VF, and rotor core size were obtained from published data (see *SI* for references), as well as from experiments performed by us. Details can be found in SI. We used FitzHugh–Nagumo kinetics to construct models of 2D, $L \times L$, sections of $L^3$ hearts and to simulate rotors in species of different sizes. $L$ refers here to the size of the model with 1, 2, 4, 8, and 16 cm used. Please refer to SI for details.

**ACKNOWLEDGMENTS.** We thank Dr. Sandeep Pandit and Dr. Elena Tolkacheva for sharing their data with us. This work was supported by National Heart, Lung, and Blood Institute Grants P01-HL087226, P01-HL39707, R01-HL70074, R01-HL 80159 (to J.J.), and R01-HL087055; an American College of Cardiology Foundation/GE Healthcare Career Development Award (to J.K.); and an American Heart Association postdoctoral fellowship (to M.C.).

1. Wiggers C (1940) *Am Heart J* 20:399–422.
2. Moe GK, Rheinboldt WC, Abildskov JA (1964) *Am Heart J* 67:200–220.
3. Moe G (1962) *Arch Int Pharmacodyn* 140:183–188.
4. Samie FH, Berenfeld , Anumonwo J, Mironov SF, Udassi S, Beaumont J, Taffet S, Pertsov AM, Jalife J (2001) *Circ Res* 89:1216–1223.
5. Schmidt-Nielsen K (1984) in *Scaling: Why Is Animal Size So Important?* (Cambridge Univ Press, Cambridge, UK).
6. West GB, Brown JH, Enquist BJ (1997) *Science* 276:122–126.
7. West GB, Brown JH, Enquist BJ (1999) *Science* 284:1677–1679.
8. Noujaim SF, Lucca E, Munoz V, Persaud D, Berenfeld O, Meijler FL, Jalife J (2004) *Circulation* 110:2802–2808.
9. Gunther B, Morgado E (1997) *Biol Res* 30:167–170.
10. Calder WA, III (1984) in *Size, Function and Life History* (Harvard Univ Press, Cambrige, MA).
11. Popovic ZB, Sun JP, Yamada H, Drinko J, Mauer K, Greenberg NL, Cheng Y, Moravec CS, Penn MS, Mazgalev TN, Thomas JD (2005) *J Physiol* 568:255–265.
12. Durrer D, van Dam RT, Freud GE, Janse MJ, Meijler FL, Arzbaecher RC (1970) *Circulation* 41:899–912.
13. Noujaim SF, Pandit SV, Berenfeld O, Vikstrom K, Cerrone M, Mironov S, Zugermayr M, Lopatin AN, Jalife J (2007) *J Physiol* 578:315–326.
14. Xu H, Guo W, Nerbonne JM (1999) *J Gen Physiol* 113:661–678.
15. Zicha S, Moss I, Allen B, Varro A, Papp J, Dumaine R, Antzelevich C, Nattel S (2003) *Am J Physiol Heart Circ Physiol* 285:H1641–H1649.
16. Varro A, Lathrop DA, Hester SB, Nanasi PP, Papp JG (1993) *Basic Res Cardiol* 88:93–102.
17. Ten Tusscher KH, Hren R, Panfilov AV (2007) *Circ Res* 100:e87–e101.

18. Nash MP, Mourad A, Clayton RH, Sutton PM, Bradley CP, Hayward M, Paterson DJ, Taggart P (2006) *Circulation* 114:536–542.
19. Panfilov AV (2006) *Heart Rhythm* 3:862–864.
20. White CR, Seymour RS (2003) *Proc Natl Acad Sci USA* 100:4046–4049.
21. West GB, Woodruff WH, Brown JH (2002) *Proc Natl Acad Sci USA* 99:2473–2478.
22. Winfree AT (1994) *Science* 266:1003–1006.
23. Jalife J, Gray RA, Morley GE, Davidenko JM (1998) *Chaos* 8:79–93.
24. Samie FH, Mandapati R, Gray RA, Watanabe Y, Zuur C, Beaumont J, Jalife J (2000) *Circ Res* 86:684–691.
25. van der Tweel LH, Strackee J, Stokhof AA, Wassenaar C, Meijler FL (1999) *J Cardiovasc Electrophysiol* 10:168–173.
26. Kleber AG, Rudy Y (2004) *Physiol Rev* 84:431–488.
27. Meijler FL, Strackee J, Stokhof AA, Wassenaar C (2002) *J Cardiovasc Electrophysiol* 13:826–830.
28. Waldo AL, Camm AJ, deRuyter H, Friedman PL, MacNeil DJ, Pauls JF, Pitt B, Pratt CM, Schwartz PJ, Veltri EP (1996) *Lancet* 348:7–12.
29. The Cardiac Arrhythmia Suppression Trial (CAST) Investigators (1989) *N Engl J Med* 321:406–412.